Uncertain Darcy's problem and the stochastic particle transport

Giacomo Garegnani
Supervisors: Dr. Sebastian Krumscheid and Prof. Fabio Nobile

Contents

1 Expected exit time from a domain **1**
1.1 Numerical Methods . . . 1
1.1.1 Discrete Euler-Maruyama . . . 1
1.1.2 Continuous Euler-Maruyama. . . . 2
1.1.3 Reflecting boundaries . . . 3
1.1.4 An adaptive procedure . . . 3
1.2 A PDE approach . . . 3
1.3 One-Dimensional Case . . . 4
1.3.1 Analytical expression of the mean exit time . . . 4
1.3.2 Numerical experiments - Estimation of τ . . . 5
1.3.3 Numerical approximation of Φ with the PDE approach . . . 6
1.3.4 Numerical experiments - Estimation of Φ . . . 8
1.4 Two-dimensional case . . . 8
1.4.1 Numerical experiments - Estimation of τ . . . 8
1.4.2 Numerical experiments - Estimation of Φ . . . 9
1.4.3 Numerical experiments - Adaptivity . . . 11

2 The uncertain Darcy problem **11**
2.1 Problem statement . . . 11
2.2 Finite Elements solution of the Darcy problem . . . 12
2.3 Solution of the SDE . . . 13
2.4 Summary . . . 14
2.5 Theoretical investigation . . . 15
2.5.1 Analysis of perturbed SDEs . . . 15
2.5.2 Analysis of numerical convergence . . . 17
2.5.3 Numerical confirmation of the theory . . . 19
2.6 Estimation of the exit time . . . 20

1 Expected exit time from a domain

We aim to estimate the exit time of a particle driven by a deterministic transport field and a stochastic diffusion from a domain $D \subset \mathbb{R}^d$. Given a vector $W(t)$ of m independent Brownian motions and two functions $f\colon \mathbb{R}^d \to \mathbb{R}^d, g\colon \mathbb{R}^d \to \mathbb{R}^{d\times m}$, we consider the following stochastic differential equation (SDE)

$$\begin{cases} dX(t) = f(X(t))dt + g(X(t))dW(t), & 0 < t \leq T, \\ X(0) = X_0, & X_0 \in D. \end{cases} \tag{1}$$

The problem is completed with two different types of boundary conditions, namely

i. *killing boundaries*: if the particle exits D the process is stopped,

ii. *reflecting boundaries*: the particle trajectory is reflected normally inside D when it touches the boundary ∂D.

Our aim is to estimate numerically the first exit time of the solution $X(t)$ from D, *i.e.*, the quantity

$$\tau = \min\{\min\{t\colon X(t) \notin D\}, T\}. \tag{2}$$

Let us remark that the parameter τ is meaningful only if there exists a portion of the boundary $\Gamma_k \subset \partial D$ that is endowed with killing boundary conditions. Otherwise, the process $X(t)$ will stay in D for the whole time interval, giving as a result $\tau = T$ for each realisation of $X(t)$. Another quantity of interest is defined as follows

$$\phi = \phi(T, X_0, F) = \mathbb{1}_{\{\tau<T\}} F(X(T)), \tag{3}$$

where $F\colon \mathbb{R}^d \to \mathbb{R}$ is a smooth function. An interesting choice of F could be the function mapping every x of $\mathbb{R}^d$ to the value 1. In this case, the expecation of ϕ is equal to the probability for $X(t)$ to exit the domain before the final time T. Let us choose the notation $F = 1$ in this case, getting

$$\Phi(T, X_0) = \mathbb{E}(\phi(T, X_0, 1)) = \Pr(\tau < T | X(0) = X_0) \tag{4}$$

In the case of general f, g and for a d-dimensional SDE, there is no closed form for τ and ϕ. Therefore, we approximate the value of τ by means of two numerical schemes, briefly presented in the following.

1.1 Numerical Methods

1.1.1 Discrete Euler-Maruyama

Given $N \in \mathbb{N}$ let us define a partition of $[0, T]$ as $P_h = \{t_i\}_{i=0}^N, t_i = ih, h = T/N$. The Discrete Euler-Maruyama method (DEM) for problem (1) is defined as follows

$$\begin{cases} X_h^d(t_{i+1}) = f(X(t_i))h + g(X(t_i))(W(t_{i+1}) - W(t_i)), \\ X_h^d(0) = X_0. \end{cases} \tag{5}$$

The exit time τ is approximated with the quantity τ_h^d defined as

$$\tau_h^d = \min\{\min\{t_i\colon X_h^d(t_i) \notin D\}, T\}. \tag{6}$$

We approximate analogously ϕ as

$$\phi_h^d = \mathbb{1}_{\{\tau_h^d<T\}} F(X_h^d(T)). \tag{7}$$

Let us state two results concerning the weak error of this method.

Proposition 1.1. *Under appropriate assumptions of smoothness of $f, g, D, \partial D, F$,*

$$|\mathbb{E}(\tau_h^d) - \mathbb{E}(\tau)| = O(\sqrt{h}). \tag{8}$$

Proposition 1.2. *Under approprate assumptions of smoothness of $f, g, D, \partial D, F$,*

$$|\mathbb{E}(\phi_h^d) - \mathbb{E}(\phi)| = O(\sqrt{h}). \tag{9}$$

An discussion of result 1.1 can be found in [6], its proof in [4]. A proof of 1.2 can be found in [2].

Algorithm 1: Continuous Euler-Maruyama

for $t_i \in P_h$ **do**
  $X(t_{i+1}) = f(X(t_i))h + g(X(t_i))(W(t_{i+1}) - W(t_i))$;
  if $X(t_{i+1}) \notin D$ **then**
    $\tau_h^c = t_{i+1}$;
    $\phi_h^c = F(X_h^c(t_{i+1}))$;
    return;
  else
    compute $p = p(x_i, x_{i+1}, h)$;
    simulate $u \sim \text{Unif}(0, 1)$;
    if $u < p$ **then**
      $\tau_h^c = t_{i+1}$;
      $\phi_h^c = F(X_h^c(t_{i+1}))$;
      return;
    end
  end
end

1.1.2 Continuous Euler-Maruyama.

Let us consider the partition P_h of $[0, T]$ as above. The Continuous Euler-Maruyama (CEM) method is defined as

$$\begin{cases} X_h^c(t) = f(X(t_i))(t - t_i) + g(X(t_i))(W(t) - W(t_i)), & t_i < t \leq t_{i+1}, \\ X_h^c(0) = X_0. \end{cases} \tag{10}$$

Let us remark that in case the particle does not exit the domain, $X_h^c(t_i) = X_h^d(t_i)$ for all $t_i \in P_h$. It is possible to compute the probability that a particle has exited the domain at a time t between two consecutive timesteps t_i, t_{i+1} when D is an half-space with the following formula [3]

$$\Pr(\exists t \in [t_i, t_{i+1}] \quad X_h^d(t) \notin D | X_h^d(t_i) = x_i, X_h^d(t_{i+1}) = x_{i+1}) = p(x_i, x_{i+1}, h), \tag{11}$$

with $p(x_i, x_{i+1}, h)$ given by

$$p(x_i, x_{i+1}, h) = \exp\Big(-2 \frac{[n \cdot (x_i - z_i)][n \cdot (x_{i+1} - z_i)]}{hn \cdot (gg^T(x_i)n)} \Big), \tag{12}$$

where z_i is the projection of x_i on ∂D and n is the normal to ∂D in z_i. At each timestep t_{i+1} we compute the probability $p(x_i, x_{i+1}, h)$, and then simulate a variable U distributed uniformly in the interval $[0, 1]$, thus obtaining a realization u. Hence, we counclude that the particle has left the domain for a time t in (t_i, t_{i+1}) if u is smaller than p. Therefore, we approximate the exit time as

$$\tau_h^c = \min\{T, \min\{t_i = hi \colon X_h(t_i) \notin D\}, \min\{t_i = hi \colon u < p(x_{i-1}, x_i, h)\}\}, \tag{13}$$

In the same way as in DEM, we can approximate ϕ as

$$\phi_h^c = \mathbb{1}_{\{\tau_h^c < T\}} F(X_h^c(T)). \tag{14}$$

We show the pseudocode for the implementation of CEM in Algorithm 1.
The weak error of this method has been studied exhaustively in previous work.

Proposition 1.3. *Under appropriate smoothness assumptions,*

$$|\mathbb{E}(\phi_h^c) - \mathbb{E}(\phi)| = O(h). \tag{15}$$

A proof of result 1.3 can be found in [3].

1.1.3 Reflecting boundaries

The reflecting boundaries are treated in the same way for both DEM and CEM. Let us denote by Γ_k and Γ_r the killing and reflecting subsets of ∂D, *i.e.*

$$\Gamma_r \cup \Gamma_k = \partial D, \quad \Gamma_r \cap \Gamma_k = \emptyset \tag{16}$$

In case the particle approaches Γ_k the exit is treated as above. If for a timestep of $t_i \in P_h$, $X(t_i)$ is not in D and has crossed Γ_r at a time $t_{i-1} < t < t_i$, we update the solution to be the normal reflection inside D of $X(t_i)$.

1.1.4 An adaptive procedure

Let us consider the function g in (1) to be fixed to a real constant σ. The numerical methods we presented can be completed with an adaptive procedure for the step size h [1]. In this frame, adaptivity is performed with respect to the position of the numerical solution $X_h(t_i)$, *i.e.*, the step size is reduced if the solution is near to the boundary of the domain D. If we denote by d_i the distance between $X_h(t_i)$ and its normal projection on ∂D, by $l \in \mathbb{N}$ a fixed parameter and by h_0 a maximum bound for h, the step size is chosen using the following formula

$$h = \max\left\{2^{-2l}h_0, \min\left\{2^{-l}h_0, \left(\frac{d}{(l+3)\sigma}\right)^2\right\}\right\}. \tag{17}$$

This formula is equivalent to dividing the domain D in three zones, in particular

- an interior zone where $h = h_{int} = 2^{-l}h_0$,
- a boundary zone where $h = h_{bound} = 2^{-2l}h_0$,
- an intermediate zone where $h = \left(\frac{d}{(l+3)\sigma}\right)^2$.

Since the loss of 0.5 in the weak order of convergence of Euler-Maruyama is due to the non-detected exits from the domain D, refining the step size only near to the boundary could lead to an error equal to the one obtained using h_{bound} on the whole domain.

1.2 A PDE approach

It is possible to express the mean exit time and the probability of exit from a domain in terms of the solution of partial differential equations (PDE's). Let us denote by Γ_k, Γ_r the killing and reflecting subsets of ∂D. We consider then the expectation of the exit time from the domain D for a trajectory that at $t = 0$ is at position x, *i.e.*,

$$\bar{\tau}(x) = \mathbb{E}(\tau | X(0) = x). \tag{18}$$

Let us define the operator $\mathcal{L}$ induced by (1) acts on a function $u\colon \mathbb{R}^d \to \mathbb{R}$ as follows

$$\mathcal{L}u = f \cdot \nabla u + \frac{1}{2} g g^T : \nabla\nabla u, \tag{19}$$

where the : operator between two matrices A, B in $\mathbb{R}^{d\times d}$ is defined as follows

$$A : B = \sum_{i,j=1}^{d} \{A\}_{ij}\{B\}_{ij} = \mathrm{tr}(A^T B). \tag{20}$$

The following result allows computing the mean exit time as the solution of an appropriate PDE.

Proposition 1.4. *Let $\mathcal{L}$ be the differential operator defined as* (19)*. Then, if Γ_k and Γ_r are respectively the killing and reflecting subsets of ∂D, such that $\Gamma_k \cup \Gamma_r = \partial D, \Gamma_k \cap \Gamma_r = \emptyset$, the mean*

exit time $\bar{\tau}(x)$ *for the solution* $X(t)$ *of* (1) *with* $X_0 = x$ *is the solution of the following boundary value problem*

$$\begin{cases} \mathcal{L}\bar{\tau}(x) = -1, & \text{in } D, \\ \bar{\tau}(x) = 0, & \text{on } \Gamma_k, \\ \nabla\bar{\tau}(x) \cdot n = 0, & \text{on } \Gamma_r, \end{cases} \tag{21}$$

where n *is the normal to* Γ_r.

Further analytical treatement of the mean exit time can be found in [8, 10].
We now consider the probability of exit from D for a solution $X(t)$ that is equal to x for $t = s < T$. This probability is the solution of a boundary value problem.

Proposition 1.5. *Let* $\mathcal{L}$ *be the differential operator defined as* (19). *Then, if* Γ_k *and* Γ_r *are respectively the killing and reflecting subsets of* ∂D, *such that* $\Gamma_k \cup \Gamma_r = \partial D, \Gamma_k \cap \Gamma_r = \emptyset$

$$\Pr(\tau < T | X(s) = x) = \Phi(x, s, T) \tag{22}$$

where $\Phi(x, t, T)$ *is the solution of the following backwards PDE*

$$\begin{cases} \dfrac{\partial}{\partial t}\Phi(x,t,T) + \mathcal{L}\Phi(x,t,T) = 0 & \text{in } D, s \le t < T, \\ \Phi(x,t,T) = 1 & \text{on } \Gamma_k, s \le t \le T, \\ \nabla\Phi(x,t,T) \cdot n = 0, & \text{on } \Gamma_r, s \le t \le T, \\ \Phi(x,T,T) = 0 & \text{in } D, \end{cases} \tag{23}$$

where n *is the normal to* Γ_r.

The proof in case $\Gamma_k = \partial D$ of this result can be found in [13]. Further treatment in case of mixed boundary conditions and the closed form of the solution for some particular geometries of $D \subset \mathbb{R}^2$ can be found in [5]. It is therefore possible to approximate $\bar{\tau}$ and Φ by means of classical methods for solving PDE's numerically, such as finite differences or the Finite Elements Method.

1.3 One-Dimensional Case

We consider problem (1) in case $d = 1$. Given $f, g \colon \mathbb{R} \to \mathbb{R}$, an interval $D = [l, r]$ and a Brownian motion $W(t)$, let us consider the following one dimensional SDE

$$\begin{cases} dX(t) = f(X(t))dt + g(X(t))dW(t), & 0 < t \le T, \\ X(0) = X_0, & X_0 \in D. \end{cases} \tag{24}$$

In this case, the boundary of D consists of the two points $\{l, r\}$. In order for the problem of the determination of τ to be meaningful, at least one of the two points should be endowed with a killing boundary condition.

1.3.1 Analytical expression of the mean exit time

In this simple frame, it is possible to deduce an analytical solution $\bar{\tau}$ of (21). Let us consider the boundary condition at $x = l$ fixed as *killing* and vary the boundary condition at $x = r$. Since the scope is deducing the exit time of a particle from D, this assumption is plausible. In this frame, it is possible to rewrite (21) as

$$\begin{cases} f(x)\bar{\tau}'(x) + \dfrac{1}{2}g^2(x)\bar{\tau}''(x) = -1, & l < x < r, \\ \bar{\tau}(l) = 0, & \\ \bar{\tau}(r) = 0, & \text{if for } x = r \text{ the boundary is } \textit{killing}, \\ \bar{\tau}'(r) = 0, & \text{if for } x = r \text{ the boundary is } \textit{reflecting}. \end{cases} \tag{25}$$

It is possible to show [8, 10] that $\bar{\tau}$ is in the one-dimensional case given by

$$\bar{\tau}(x) = -2\int_l^x \exp(-\psi(z)) \int_l^z \frac{\exp(\psi(y))}{g^2(y)} dy + c_1 \int_l^x \exp(-\psi(y)) dy + c_2, \tag{26}$$

where the function ψ is defined as

$$\psi(x) = \int_l^x \frac{2f(y)}{g^2(y)} dy, \tag{27}$$

and the constants $c_1, c_2 \in \mathbb{R}$ depend on the boundary conditions as follows

$$\begin{aligned} &c_1 = 2\frac{\int_l^r \exp(-\psi(z)) \int_l^z \frac{\exp(\psi(y))}{g^2(y)} dy}{\int_l^r \exp(-\psi(y)) dy}, \text{ if for } x = r \text{ the boundary is } \textit{killing}, \\ &c_1 = 2\int_l^r \frac{\exp(-\psi(y))}{g(y)^2} dy, \text{ if for } x = r \text{ the boundary is } \textit{reflecting}, \\ &c_2 = 0. \end{aligned} \tag{28}$$

Let us remark that in case $f = -V'$ for some smooth function V and $g = \sigma \in \mathbb{R}$, the expression of ψ semplifies to

$$\psi(x) = 2\frac{V(l) - V(x)}{\sigma^2}. \tag{29}$$

The value for the expected exit time given by (26) will be used as a reference for verifying the order of convergence of the numerical methods.

1.3.2 Numerical experiments - Estimation of τ

Smooth case. We consider as a domain for (24) the interval $D = [-1, 1]$, final time $T = 5$ and the following functions

$$\begin{aligned} &f(x) = -V'(x), \text{ where } V(x) = 0.1(8x^4 - 8x^2 + x + 2), \\ &g(x) = \sigma = 3. \end{aligned} \tag{30}$$

We approximate the value of τ with a Montecarlo simulation of τ_h^d and τ_h^c computed as in (6) and (13) from the solutions provided by DEM and CEM respectively. In order to verify the order of convergence of the methods, we let N vary in the set $2^i, i = 3, \ldots, 12$ and we fix the number of trajectories M to 10000. In this way, the error caused by the Montecarlo estimation should not spoil the order of convergence. In Figure 1 we show the errors obtained fixing $X_0 = 0$ in both the cases of killing and reflecting boundary conditions in $x = 1$. Moreover, in Figure 2 we show an approximation of τ obtained with the two methods with $h = T/128$ and $M = 1000$ for a set of 10 initial values equispaced along D. It is possible to remark that computing the probability of exit between two consecutive timesteps as in (12) allows correcting the overestimation of τ obtained simply using DEM. We want to estimate the computational time for both the method. We consider $M = 10000$, killing boundary conditions and $N = 2^i, i = 3, \ldots, 12$. We remark that the computational time required by CEM is higher than for DEM if the same value of h is employed. On the other hand, fixing the error, CEM is faster than DEM in this case.

Rough case. We consider the same domain D as above, $T = 5$ and $g = \sigma = 3$. We consider V to be piecewise linear, so that $f = -dV$ is piecewise constant. In particular, we choose the following form for V

$$V = 0.1 \begin{cases} -2x - 1, & x < -0.5, \\ 4x + 2, & -0.5 \le x < 0, \\ -2x + 2, & 0 \le x < 0.5, \\ 4x - 1, & x \ge 0.5. \end{cases} \tag{31}$$

This is a linear interpolation of the function V we used in the smooth case above in the points $\{-1, -0.5, 0, 0.5, 1\}$. This case is of particular interest, since if the function f is the result of a

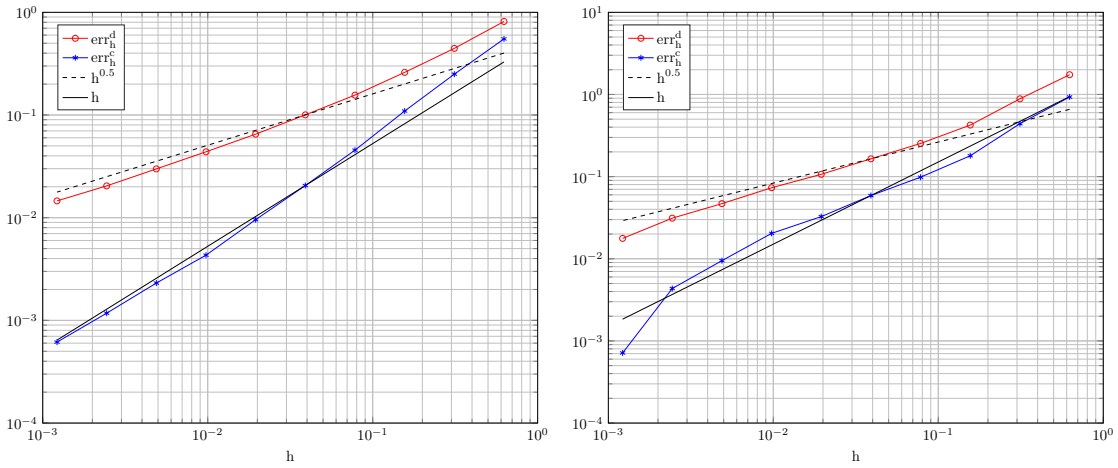

(a) Killing boundary in $x = 1$ (b) Reflecting boundary in $x = 1$

Figure 1: Approximation of τ. Orders of convergence for DEM and CEM in the one-dimensional case.

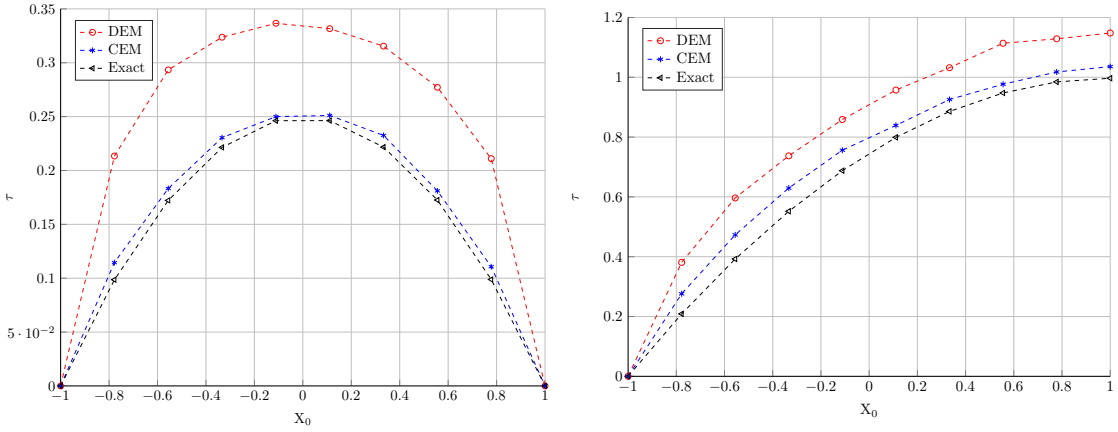

(a) Killing boundary in $x = 1$ (b) Reflecting boundary in $x = 1$

Figure 2: Approximation of τ as a function of the initial value X_0.

numerical method on a PDE, it could not be smooth as in the previous case. We perform DEM and CEM with the same parameters as before, *i.e.*, $M = 10000, N = 2^i, i = 3, \ldots, 12$. In Figure 3 it is possible to remark that the rate of convergence of DEM is unvaried with respect to the previous case. The CEM method experiences a slight decrease in the order of convergence with respect to the smooth case.

1.3.3 Numerical approximation of Φ with the PDE approach

Let us consider D as the interval $[l, r]$, the boundary condition in l to be fixed to killing and in r to be either killing or reflecting. In this case and for f independent of t and $g = \sigma \in \mathbb{R}$ (23) can

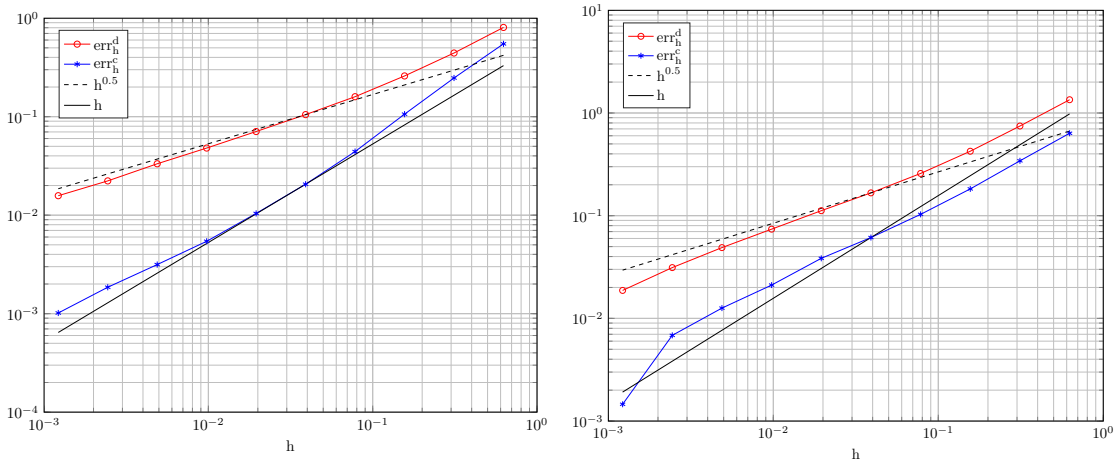

(a) Killing boundary in $x = 1$

(b) Reflecting boundary in $x = 1$

Figure 3: Approximation of τ. Orders of convergence for DEM and CEM in the one-dimensional case with f piecewise constant.

be written as the following initial value PDE

$$\begin{cases} -\dfrac{\partial}{\partial t}\Phi(t,x) + f\dfrac{\partial}{\partial x}\Phi(t,x) + \dfrac{1}{2}\sigma^2\dfrac{\partial^2}{\partial x^2}\Phi(t,x) = 0, & l < x < r \\ \Phi(t,l) = 1, & \\ \Phi(t,r) = 1, & \text{if for } x = r \text{ the boundary is } \textit{killing} \\ \dfrac{\partial}{\partial x}\Phi(t,r) = 0, & \text{if for } x = r \text{ the boundary is } \textit{reflecting} \\ \Phi(0,x) = 0. & \end{cases} \tag{32}$$

This equation can be solved, *e.g.*, using finite differences. We employ the theta method for solving (32). Let us consider the case in which r is a killing boundary, *i.e.*, the PDE is endowed with Dirichlet boundary conditions. Given a step size Δ_t for time integration and an uniform grid $x_i = l + i\Delta_x, i = 0, \ldots, N+1, x_{N+1} = r$, at each timestep k one has to find the solution of the linear system

$$(I - \Delta_t\theta A)u^{k+1} = (I + \Delta_t(1-\theta)A)u^k + hF,\ 0 \le \theta \le 1, \tag{33}$$

where I is the identity matrix of $\mathbb{R}^{N\times N}$. The matrix A of $\mathbb{R}^{N\times N}$ and the vector F of $\mathbb{R}^N$ define the space discretization and the boundary conditions and are defined by

$$A = \frac{1}{2\Delta_x}\begin{pmatrix} \alpha_1 & \beta_1 & & \\ \gamma_1 & \alpha_2 & \beta_2 & \\ & \ddots & \ddots & \ddots \end{pmatrix}, \quad F = \frac{1}{2\Delta_x}\begin{pmatrix} F_1 \cdots F_N \end{pmatrix}^T \tag{34}$$

and the coefficients are given by

$$\begin{aligned} \alpha_i &= -\frac{2\sigma^2}{\Delta_x},\ i = 1, \ldots, N, \\ \beta_i &= \frac{\sigma^2}{\Delta_x} + f(x_i),\ i = 1, \ldots, N-1, \\ \gamma_i &= \frac{\sigma^2}{\Delta_x} - f(x_{i+1}),\ i = 1, \ldots, N-1, \\ F_1 &= \frac{\sigma^2}{\Delta_x} - f(x_1), \\ F_N &= \frac{\sigma^2}{\Delta_x} - f(x_{N-1}). \end{aligned} \tag{35}$$

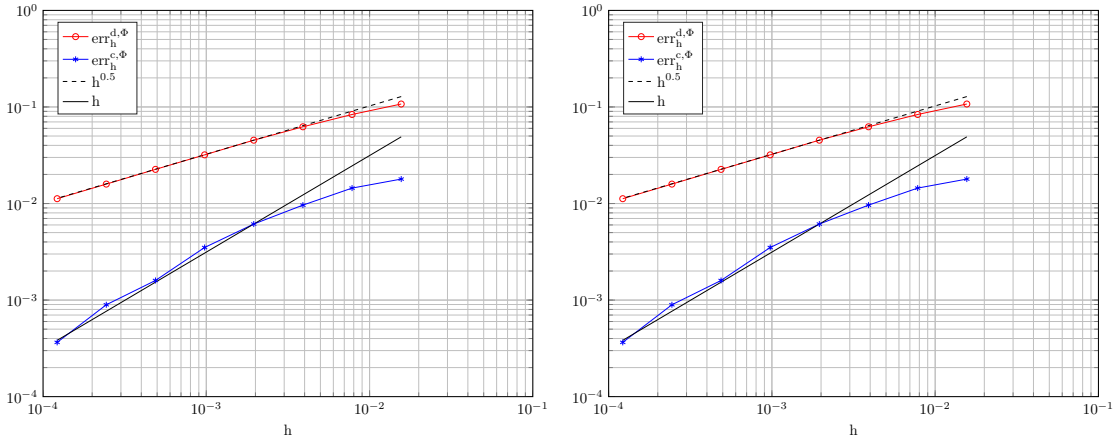

(a) Killing boundary in $x = 1$

(b) Reflecting boundary in $x = 1$

Figure 4: Approximation of Φ. Orders of convergence of DEM and CEM in the one-dimensional case.

The case of reflecting boundary condtion in $x = r$ is similar and affects only the computation of the matrix A and the vector F. In particular, we introduce a *ghost node* at position $x = r + \Delta_x$, compute the derivative using a centrate approximation and impose that it is equal to 0, which leads to the condition that the value in the node in $x = r$ is equal to the value in $x = r - \Delta_x$. Since the matrix defining the system (33) is tridiagonal, one can choose Δ_t, Δ_x to be small and obtain a precise solution of (32) in a reasonable computational time. In the following, we will compare the values given by Montecarlo simulations using DEM and CEM with the solution of the theta method with $\theta = 0.5$.

1.3.4 Numerical experiments - Estimation of Φ

Smooth case. We consider (24) with $D = [-1, 1]$, the final time $T = 0.5$ and we define

$$\begin{aligned} f(x) &= -V'(x), \text{ where } V(x) = 8x^4 - 8x^2 + x + 2, \\ g(x) &= \sigma = 2. \end{aligned} \tag{36}$$

In order to approximate Φ, we perform a Montecarlo simulation using both DEM and CEM, with $M = 6 \cdot 10^5$ trajectories in order to kill the statistical error. We consider the number of timesteps for the time integration to be $N = 2^i, i = 5, \ldots, 12$. Numerical results (Figure 4a) confirm that the weak error for DEM is of order 0.5, while for CEM the order of convergence is 1.

1.4 Two-dimensional case

We are interested in estimating the exit time of a particle from a domain $D \subset \mathbb{R}^2$. Given $W(t)$ a vector of two independent Brownian motions, we consider the equation (1). In this case, $f \colon \mathbb{R}^2 \to \mathbb{R}^2, g \colon \mathbb{R}^2 \to \mathbb{R}^{2\times 2}$. We compute the mean exit time and the exit probability using DEM and CEM and compare results with the numerical solution of the PDE's presented in 1.2.

1.4.1 Numerical experiments - Estimation of τ

Killing boundary conditions. We consider a simple case of (1) in $D = [-1, 1] \times [-1, 1]$, where

$$f = 0 \in R^2, \; g = \sigma I \in R^{2\times 2}, \sigma \in \mathbb{R}.$$

Moreover, we consider ∂D to be a killing boundary. The solution in this case is a Brownian motion. In this case, the partial differential equation (21) reduces to

$$\begin{cases} -\sigma^2 \Delta \bar{\tau} = 2, & \text{in } D, \\ \bar{\tau} = 0, & \text{on } \partial D. \end{cases} \tag{37}$$

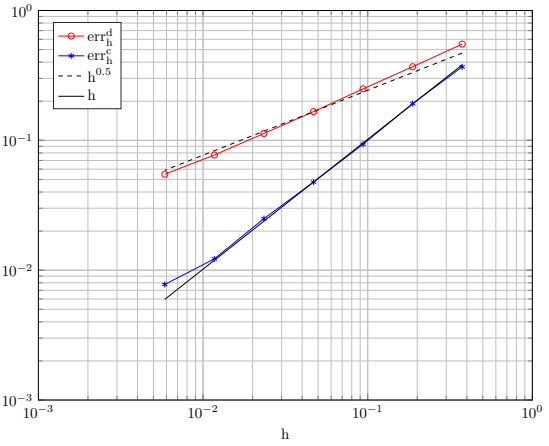

(a) Convergence of CEM and DEM.

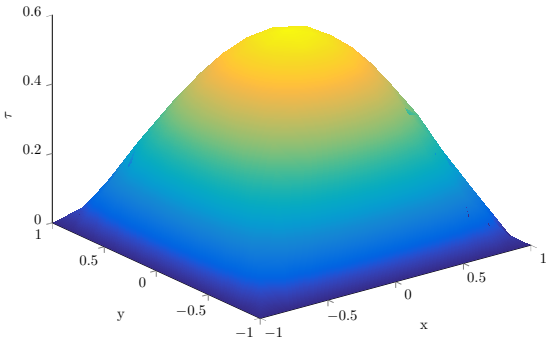

(b) Expectation of exit time.

Figure 5: Summary of the results for τ in the two-dimensional case with pure killing boundary conditions.

This is the Poisson equation, hence it is possible to solve it numerically with the Finite Elements Method or the finite differences avoiding a high computational cost. We use the Finite Elements Method adopting a regular mesh with equal constant spacing in the x and y directions, obtaining a solution as in Figure 5b. In order to verify the orders of convergence of DEM and CEM, we set $T = 3$, $\sigma = 1$, $X_0 = (0,0)^T$, with $M = 10000$ and $N = 2^i, i = 3, \dots, 9$. We then compare the Montecarlo estimation we obtain with the value of $\bar{\tau}$ in $(0,0)$, obtained by interpolation on the Finite Elements solution. The orders of convergence for this numerical experiment are shown in Figure 5a. The results confirm the theoretical orders of convergence for DEM and CEM, with an average order of 0.55 for DEM and 0.93 for CEM, which corrects to 0.98 if the last point is not taken into account.

Mixed boundary conditions. We consider the same problem as above with mixed killing and reflecting boundary conditions. f and g are the same as above, so the SDE model does not change, but we consider the two left and right boundaries of D, defined by $x = \pm 1$, to be reflecting. We denote this portion of the boundary as Γ_r, and the rest as Γ_k. In this case, the equation for $\bar{\tau}$ becomes

$$\begin{cases} -\sigma^2 \Delta \bar{\tau} = 2, & \text{in } D, \\ \bar{\tau} = 0, & \text{on } \Gamma_k, \\ \partial \bar{\tau} \cdot n = 0, & \text{on } \Gamma_r. \end{cases} \tag{38}$$

The solution of this equation is shown in Figure 6b. We compute the expectation of τ with DEM and CEM with the same parameters as above. The results (Figure 6a), show that the theoretical orders of convergence are not spoilt by this choice of boundary conditions. The mean order for DEM in this case is 0.55, while for CEM it is 1.15.

1.4.2 Numerical experiments - Estimation of Φ

Killing boundary conditions. We consider the same simple case as in section 1.4.1 We consider ∂D to be a killing boundary. The solution of (1) is in this case a Brownian motion. In this case, the partial differential equation (23) reduces to

$$\begin{cases} \dfrac{\partial}{\partial t}\Phi(x,t,T) + \dfrac{1}{2}\sigma^2 \Delta \Phi(x,t,T) = 0, & \text{in } D, 0 \le t < T, \\ \Phi(x,t,T) = 1, & \text{on } \partial D, 0 \le t < T, \\ \Phi(x,T,T) = 0, & \text{in } D. \end{cases} \tag{39}$$

We solve this problem numerically with the Finite Elements Method as for (38). The solution at $t = 0$ is shown in Figure 7b. We verify the orders of convergence of DEM and CEM setting

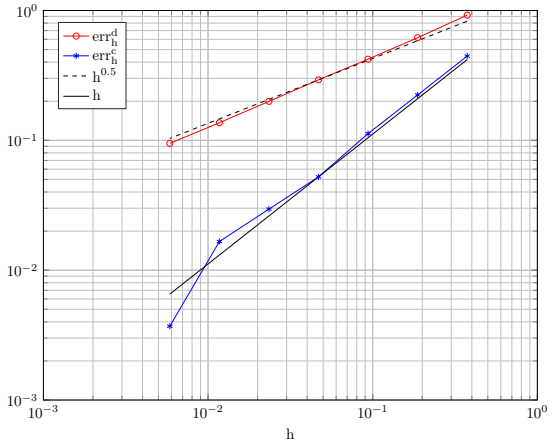

(a) Convergence of CEM and DEM.

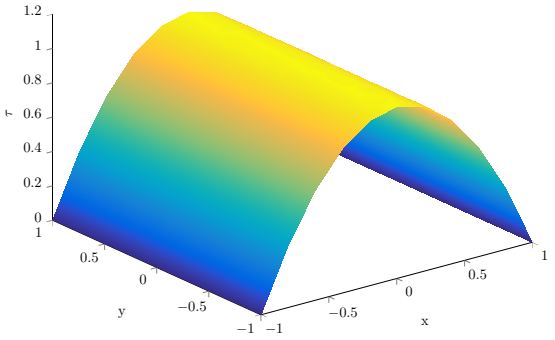

(b) Expectation of exit time.

Figure 6: Summary of the results for τ in the two-dimensional case with mixed boundary conditions.

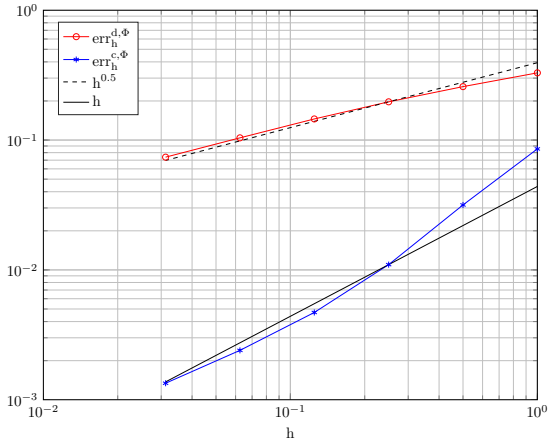

(a) Convergence of CEM and DEM.

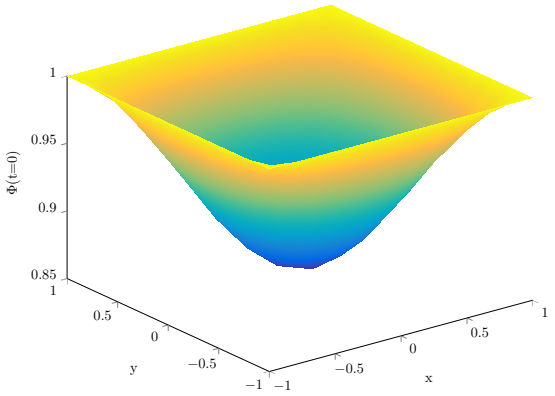

(b) Probability of exit.

Figure 7: Summary of the results for Φ in the two-dimensional case with pure killing boundary conditions.

$X_0 = (0,0)^T, \sigma = 1, T = 1$. We consider $M = 100000$ trajectories and $N = 2^i, i = 0, \ldots, 5$. We then compare the Montecarlo estimation with the value of Φ in $(0,0)$, obtained by interpolation on the Finite Elements solution. The orders of convergence for this numerical experiment are shown in Figure 7a. The theoretical orders of convergence are confirmed in this case as well, with an average order of 0.43 for DEM and 1.19 for CEM.

Mixed boundary conditions. We consider the same values for the parameters, the time integration and the Montecarlo estimation as in the pure killing case. In this case, we set the boundary conditions to be reflecting on the subset of the boundary of D defined by $x = \pm 1$ and killing for the other boundaries.Therefore, in this case the exit probability Φ is the solution of the folllowing PDE

$$\begin{cases} \dfrac{\partial}{\partial t}\Phi(x,t,T) + \dfrac{1}{2}\sigma^2\Delta\Phi(x,t,T) = 0, & \text{in } D, 0 \le t < T, \\ \Phi(x,t,T) = 1, & \text{on } \Gamma_k, 0 \le t < T, \\ \nabla\Phi(x,t,T)\cdot n = 0, & \text{on } \Gamma_r, 0 \le t < T, \\ \Phi(x,T,T) = 0, & \text{in } D. \end{cases} \tag{40}$$

The solution of this equation computed with Finite Elements is shown in Figure 8b. The convergence results for DEM and CEM are shown in Figure 8a. The mean orders in this case are 0.37

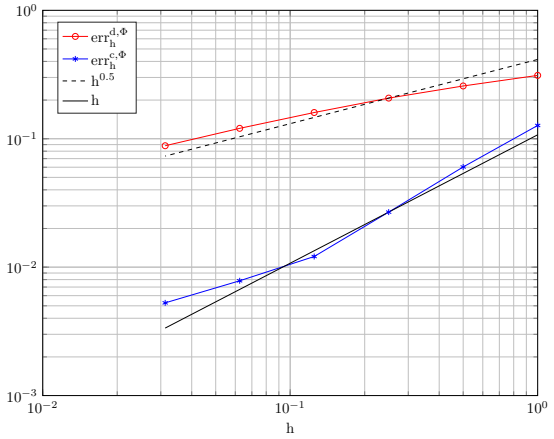

(a) Convergence of CEM and DEM.

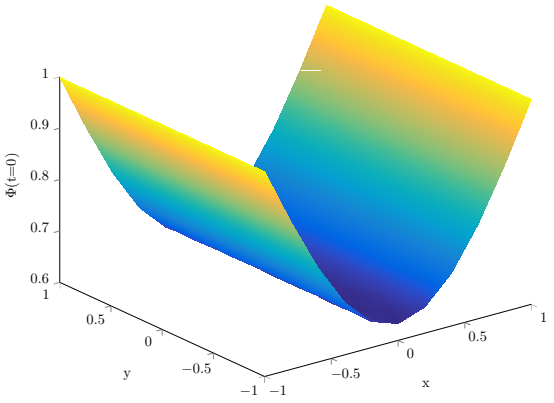

(b) Probability of exit.

Figure 8: Summary of the results for Φ in the two-dimensional case with mixed boundary conditions.

for DEM and 0.87 for CEM, which is less than the prediction given by theoretical results. This decrease in the convergence rate is remarkable for small values of h. This could mean that the error caused by the Finite Element approximation of the solution of (40) is not negligible with respect to the error of CEM.

1.4.3 Numerical experiments - Adaptivity

We apply to a test case the adaptivity procedure explained in section 1.1.4. In particular, we fix $f = 0, g = \sigma = 1, T = 3$ and $X_0 = (0,0)^T$ in the square domain $D = [0,1]^2$ with pure killing boundary conditions. We vary l in (17) in the range $l = 0, \dots, 7$ and we run three methods

1. Adaptive method with $h_0 = T$
2. DEM with $h = h_{bound}$ for each timestep
3. CEM with $h = h_{int}$ for each timestep

We expect the three methods to have an error of order $O(h_{int})$ when estimating the mean exit time. In Figure 9a it is possible to remark that the error is of the same order for the three methods. Moreover, the methods have approximately the same error, *i.e.*, the constant multipling h_{int} is the same for the three methods. In order to choose which method performs better from the point of view of computational cost, we compute the mean number of timesteps that they perform in order to estimate the exit time. From Figure 9b it is clear that CEM with h_{int} for every timestep performs better than the other two methods, with the adaptive procedure applied to DEM which implies lower computational time than DEM with constant timestep equal to h_{bound}. We can conclude that the approach based on Brownian bridge proposed in [3] has better performances when estimating the mean exit time from a domain.

2 The uncertain Darcy problem

The two methods for approximating the mean exit time have been investigated in a general frame. In the following we will consider (1) with $f\colon \mathbb{R}^2 \to \mathbb{R}^2$ given by the solution of the uncertain Darcy problem.

2.1 Problem statement

Let us consider a domain $D \subset \mathbb{R}^2$. Let us define the Neumann boundaries of D as Γ_N, its inlet boundary as Γ_{in} and its outlet boundary as Γ_{out}. Then, we search the solution of the following

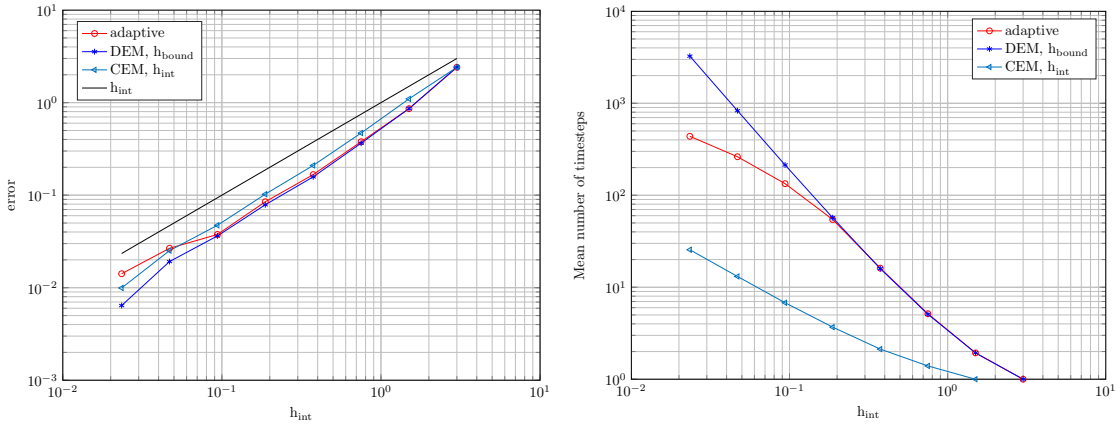

(a) Convergence of the error.

(b) Computational cost.

Figure 9: Estimation of τ in the square domain with mixed boundary conditions. Comparison between DEM with fixed or adaptive step size.

problem

$$\begin{cases} u = -A\nabla p, & \text{in } D, \\ \nabla \cdot u = 0, & \text{in } D, \\ p = p_0, & \text{on } \Gamma_{in}, \\ p = 0, & \text{on } \Gamma_{out}, \\ \nabla p = 0, & \text{on } \Gamma_N, \end{cases} \tag{41}$$

where A is a random field. The solution u of this equation is used as transport field in equation (1), which can be therefore written as

$$\begin{cases} dX(t) = u(X)dt + \sigma dW(t), & 0 < t \leq T, \\ X(0) = X_0, & X_0 \in D, \end{cases} \tag{42}$$

where we set the boundary conditions to be reflecting on Γ_N and killing on both $\Gamma_{in}, \Gamma_{out}$.

2.2 Finite Elements solution of the Darcy problem

Let us consider the domain $D = [-1, 1] \times [-1, 1]$. The random field A in (41) is chosen to be lognormal, *i.e.*,

$$A = e^{\gamma}, \tag{43}$$

where γ is a normal random field defined by its covariance function $\text{cov}_\gamma(x_1, x_2)$ for any couple of points x_1, x_2 in the domain D. The covariance function is of the Matern family, thus having the following form

$$\text{cov}_\gamma(x_1, x_2) = \frac{\sigma_A^2}{\Gamma(\nu)2^{\nu-1}} \left(\sqrt{2\nu}\frac{|x_1 - x_2|}{L_c}\right)^{\nu} K_\nu \left(\sqrt{2\nu}\frac{|x_1 - x_2|}{L_c}\right), \quad \nu \geq 0.5, \tag{44}$$

where σ_A^2 is the variance, L_c is the correlation length, Γ is the gamma function, K_ν is the modified Bessel function of the second kind and ν is a parameter. Let us remark that the covariance function does not depend on x_1, x_2 but only on their euclidean distance $|x_1 - x_2|$. The regularity of the covariance function and of the realizations of A depend on ν. In particular, for ν equal to 0.5, the covariance is Lipschitz continuous and the field is α-Hölder continuous for $\alpha < 0.5$. Results concerning further regularity properties of A can be found in [9]. The realizations of A are computed using a discrete Fourier transformation on the vertices of a grid of D, equispaced on both the x and y directions with the same spacing Δ_A. Then, the numerical solution $\hat{p}$ of (41) is obtained with linear Finite Elements on a regular mesh T_p with maximum element size Δ_p. Since the vertices of

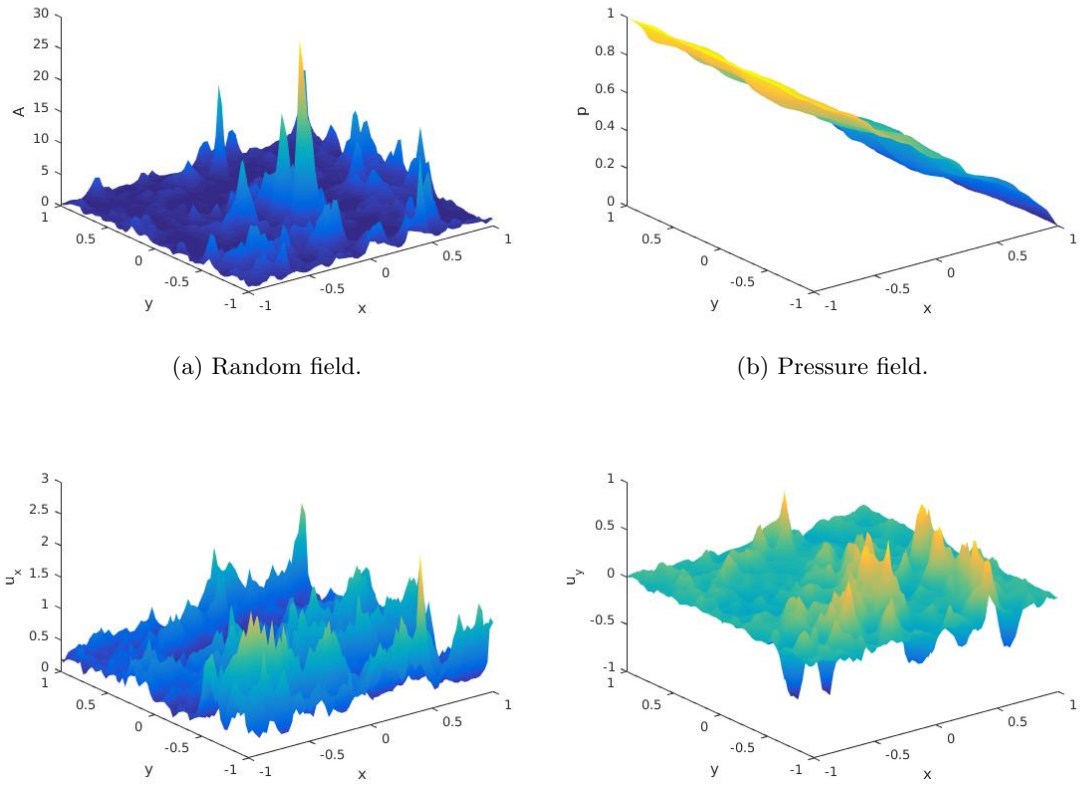

(a) Random field.

(b) Pressure field.

(c) x component of velocity field.

(d) y component of velocity field.

Figure 10: Approximate solution of the uncertain Darcy problem.

the grid on which we compute A do not coincide with the vertices of T_p, we interpolate A on T_p to obtain $\hat{p}$. Then, the velocity field $\hat{u}$ is retrived computing the gradient of $\hat{p}$. The results for a realization of A are shown in Figure 10, where the value of the inlet pressure p_0 is equal to 1, and the parameters for the random field are $\nu = 0.5, L_c = 0.05$.

2.3 Solution of the SDE

Once the Finite Element approximation $\hat{u}$ of the velocity field is available, it is possible to approximate by means of DEM and CEM the solution of (42). The values of the numerical solution X_h can take any value in D, therefore it is necessary that the velocity field is defined in any point in D. If an interpolation of $\hat{u}$ is performed at each step, both DEM and CEM lose in computational efficiency. Hence, an interpolation of $\hat{u}$ has to be performed before the numerical integration of the SDE. Therefore, we define a grid with spacing Δ_u, interpolating the values of $\hat{u}$ in the center of each square defined by the grid (Figure 11). Let us denote by Q the set of the interpolation points, whose elements are defined by

$$\{Q\}_{ij} = \big(-1 + (i - 0.5)\Delta_u, \quad -1 + (j - 0.5)\Delta_u\big)^T, \quad i, j = 1, \dots, \frac{2}{\Delta_u} =: N_u. \tag{45}$$

We compute two matrices U_x, U_y of $\mathbb{R}^{N_u \times N_u}$ containing the values of the two components of $\hat{u}$ interpolated on the points of Q. Then, the velocity field is considered to be piecewise constant in each square of the grid defined by Δ_u. Therefore, if we denote by $\tilde{u}$ the transport field for the

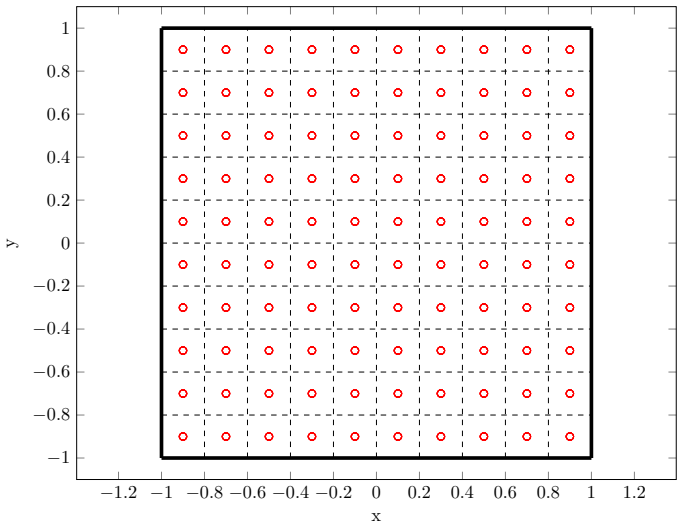

Figure 11: Grid used for interpolation of $\hat{u}$. Dots represent the interpolation points.

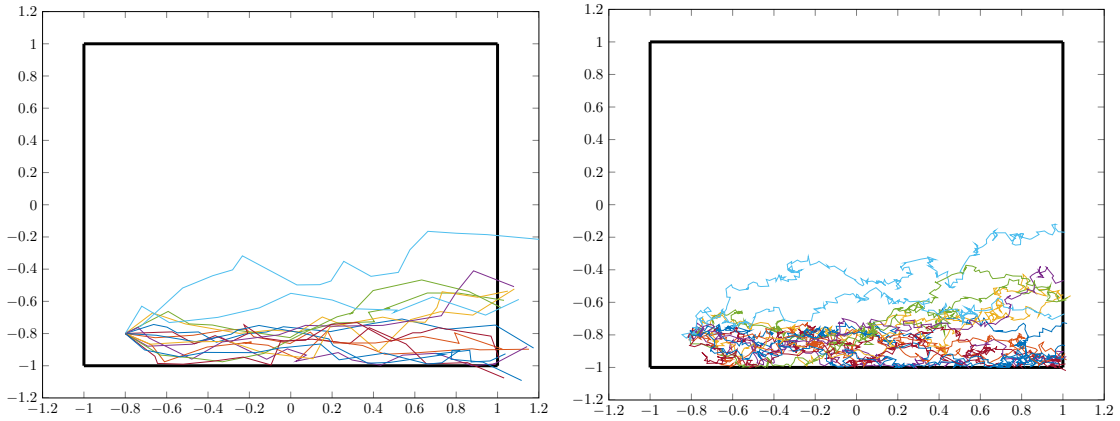

(a) Big timestep.

(b) Small timestep .

Figure 12: Trajectories of the numerical solution of (42) with DEM.

SDE, at the i-th step of the integration $\tilde{u}$ is evaluated as follows

$$\tilde{u}(X_h(t_i)) = \begin{pmatrix} U_x(\lceil (X_{h,1}(t_i)+1)/\Delta_u \rceil, \lceil (X_{h,2}(t_i)+1)/\Delta_u \rceil) \\ U_y(\lceil (X_{h,1}(t_i)+1)/\Delta_u \rceil, \lceil (X_{h,2}(t_i)+1)/\Delta_u \rceil) \end{pmatrix}, \tag{46}$$

where $X_{h,1}, X_{h,2}$ denote the first and second components of X_h and $U_x(i,j)$ represents the element (i,j) of the matrix U_x (respectively U_y). Then, given the step size h, one step of DEM will be defined as

$$X_h(t_{i+1}) = \tilde{u}(X_h(t_i))h + \sigma(W(t_{i+1}) - W(t_i)). \tag{47}$$

Given an input initial value X_0 for (42), we approximate the solution using DEM and CEM using the strategy above. In Figure 12 we display 15 trajectories for $X_0 = (-0.8, -0.8)^T$ with two different timesteps. The choice of the initial point is made in order to observe reflections on the lower boundary of the domain D on which we compute the solution, as well as the killing boundary at the right side.

2.4 Summary

Let us summarize the procedure we use for approximating the solution of (42).

1. Generate A on a grid with spacing Δ_A with a Fourier transform method.

2. Approximate the solution of (41) with the Finite Element methods on a fine triangulation T_p with maximum element size Δ_p.

3. Compute the velocity field from the FEM solution and interpolate it on a grid with spacing Δ_u to obtain a piece-wise constant field $\tilde{u}$.

4. Solve (42) with DEM or CEM to evaluate the mean exit time $\bar{\tau}$ using $\tilde{u}$ as the transport field.

2.5 Theoretical investigation

2.5.1 Analysis of perturbed SDEs

The procedure explained above could give rise to theoretical issues concerning the existence and uniqueness of the solution of (42). In particular, when performing step 3. of the procedure as in the list above, the hypothesis that the transport field of the SDE is Lipschitz continuous is not valid anymore, and therefore we have no guarantee that (42) is well-posed. On the other side, we can hope that if $\tilde{u}$ tends uniformly to the exact solution u of (41), provided that the latter is a smooth function, the solution of the SDE that has $\tilde{u}$ as a transport field tends to the solution given by u. In the following we present a result that supports our numerical procedure. Let us consider $\sigma \in \mathbb{R}$, $f\colon \mathbb{R}^d \to \mathbb{R}^d$, $W_1(t)$ a standard d-dimensional Wiener process and the following SDE

$$\begin{cases} dX(t) = f(X(t))dt + \sigma I dW_1(t), \quad 0 < t \leq T, \\ X(0) = X_0, \end{cases} \tag{48}$$

where I is the identity matrix in $\mathbb{R}^{d\times d}$. Moreover, let us consider a perturbation of the transport field $f^\varepsilon\colon \mathbb{R}^d \to \mathbb{R}^d$ and a standard d-dimensional Wiener process $W_2(t)$ not necessarily independent of $W_1(t)$. Then, we consider the perturbed SDE

$$\begin{cases} dX^\varepsilon(t) = f^\varepsilon(X^\varepsilon(t))dt + \sigma I dW_2(t), \quad 0 < t \leq T, \\ X^\varepsilon(0) = X_0. \end{cases} \tag{49}$$

Finally, let us introduce the following notation

$$\|f - f^\varepsilon\|_\infty = \sup_{x\in\mathbb{R}} |f(x) - f^\varepsilon(x)|.$$

We can state the following preliminary result

Lemma 2.1. *With the notation above, let us consider $d = 1$, $W_1 = W_2 = W$ almost everywhere. Then, given a real constant K and with the following assumptions*

1. $|f(x) - f(y)| \leq K|x - y|$, $\forall x, y \in \mathbb{R}$
2. $\|f - f^\varepsilon\|_\infty \overset{\varepsilon\to 0}{\longrightarrow} 0$,

the solution $X^\varepsilon(t)$ of (49) converges strongly to the solution $X(t)$ of (48) in $L^2(\Omega)$, i.e.

$$\mathbb{E} \sup_{0\leq t\leq T} |X^\varepsilon(t) - X(t)|^2 \overset{\varepsilon\to 0}{\longrightarrow} 0.$$

Proof. For almost all ω

$$\begin{aligned} |X^\varepsilon(t) - X(t)|^2 &= \Big| \int_0^t (f^\varepsilon(X^\varepsilon(s)) - f(X(s)))ds \Big|^2 \\ &\leq T \int_0^t |f^\varepsilon(X^\varepsilon(s)) - f(X(s))|^2 ds \\ &\leq 2T \int_0^t |f^\varepsilon(X^\varepsilon(s)) - f(X^\varepsilon(s))|^2 ds + 2T \int_0^t |f(X^\varepsilon(s)) - f(X(s))|^2 ds \\ &\leq 2T^2 \|f - f^\varepsilon\|_\infty^2 + 2T^2K^2 \int_0^t |X^\varepsilon(s) - X(s)|^2 ds. \end{aligned}$$

We then apply Gronwall's inequality, which gives

$$|X^\varepsilon(t) - X(t)|^2 \leq 2T^2 \|f - f^\varepsilon\|_\infty^2 e^{2K^2T^2}, \quad a.e. \tag{50}$$

Since the right hand side of the inequality is constant, we can then take the supremum over time and the expectation at both sides, *i.e.*,

$$\mathbb{E} \sup_{0\leq t\leq T} |X^\varepsilon(t) - X(t)|^2 \leq 2T^2 \|f - f^\varepsilon\|_\infty^2 e^{2K^2T^2}.$$

Then, assumption 2. gives the result. □

We now consider the case of two independent Wiener processes.

Lemma 2.2. *With the notation above and the assumptions 1. and 2. of Lemma 2.1, let us consider W_1 independent of W_2 and $d = 1$. Then*

$$\mathbb{E} \sup_{0\leq t\leq T} |X^\varepsilon(t) - X(t)|^2 \leq 4T(T\|f - f^\varepsilon\|_\infty^2 + 4\sigma^2)e^{2K^2T^2}.$$

Proof. Let us compute the difference between $X^\varepsilon(t)$ and $X(t)$. Applying Young's inequality, we get

$$\begin{aligned}\mathbb{E} \sup_{0\leq t\leq T} |X^\varepsilon(t) - X(t)|^2 \leq 2\mathbb{E} \sup_{0\leq t\leq T} \Big| \int_0^t (f^\varepsilon(X^\varepsilon(s)) - f(X(s)))ds\Big|^2 \\ + 2\sigma^2\mathbb{E} \sup_{0\leq t\leq T} \Big| \int_0^t dW_1(s) - \int_0^t dW_2(s)\Big|^2.\end{aligned}$$

Let us define $Z(t) := W_1(t) - W_2(t)$. $Z(t)$ is a standard Wiener process with variance $2t$, thus it is a martingale. Hence, we can apply Doob's maximal quadratic inequality (*e.g.*, [11, Page 11]) to the second term, obtaining

$$\mathbb{E} \sup_{0\leq t\leq T} \Big| \int_0^t dW_1(s) - \int_0^t dW_2(s)\Big|^2 = \mathbb{E} \sup_{0\leq t\leq T} |Z(t)|^2 \leq 4\mathbb{E}|Z(T)|^2 = 8T.$$

For the first term, we can apply the same technique as in Lemma 2.1. Therefore, we get the result

$$\mathbb{E} \sup_{0\leq t\leq T} |X^\varepsilon(t) - X(t)|^2 \leq (4T^2\|f - f^\varepsilon\|_\infty^2 + 16T\sigma^2)e^{2K^2T^2}.$$

□

With those preliminary results, we can now consider the general case of a d-dimensional SDE.

Proposition 2.1. *With the notation above and if $f\colon \mathbb{R}^d \to \mathbb{R}^d$, $f^\varepsilon\colon \mathbb{R}^d \to \mathbb{R}^d$, satisfy*

1. $\|f(x) - f(y)\| \leq K\|x - y\|$, $\forall x, y \in \mathbb{R}^d$,
2. $\|f_i - f_i^\varepsilon\|_\infty \xrightarrow{\varepsilon\to 0} 0$, $i = 1, \ldots, d$,

then it is true for $X(t), X^\varepsilon(t)$ the solutions of (48) and (49) that

$$\mathbb{E}\|X^\varepsilon(t) - X(t)\|_2^2 \leq \Big(4T^2 \sum_{i=1}^d \sup_{x\in\mathbb{R}} |f_i(x) - f_i^\varepsilon(x)|^2 + 16Td\sigma^2\Big)e^{2dK^2T^2}. \tag{51}$$

Proof. The proof follows from Lemma 2.2. Let us denote by $X_i(t), X_i^\varepsilon(t)$ the i-th component of the solution, $i = 1, \ldots, d$. Then

$$\begin{aligned}\mathbb{E}\|X^\varepsilon(t) - X(t)\|^2 &= \mathbb{E}\sum_{i=1}^d |X_i^\varepsilon(t) - X_i(t)|^2 \\ &= \sum_{i=1}^d \mathbb{E}|X_i^\varepsilon(t) - X_i(t)|^2\end{aligned}$$

Then, applying Lemma 2.2 to each component of the solution, one obtains (51). □

Remark 2.1. (Convergence considerations.) The result of Proposition 2.1 shows that in case one uses two different Wiener processes W_1, W_2 for the standard and the perturbed SDEs, the strong convergence is not granted. In fact, while the first term in estimation (51) disappears due to the uniform convergence of the perturbed transport field towards the non-perturbed one, the error due to the different Wiener processes is not disappearing with respect to ε. However, in underground flow models the variance σ of the Brownian diffusion is often small with respect to the transport field. Therefore, one could consider the solution $X^\varepsilon(t)$ of (49) to be practically converging to the solution $X(t)$ of (48).

Remark 2.2. (Interpolation results.) Let us consider a domain $D \in \mathbb{R}^d$ where f and f^ε are defined and f^ε to be a polynomial interpolation of f on D. Then, the interpolation error of can be estimated if f is regular enough. In particular, the following results are valid [12, Chapter 8] for a grid of size ε

1. f Lipschitz continuous of constant K, f^ε piecewise constant interpolation, C_0 a real constant
$$\sup_{x\in D} \|f(x) - f^\varepsilon(x)\| \leq C_0 K \varepsilon.$$
2. f of class $\mathcal{C}^1$, f^ε piecewise constant interpolation, C_1 a real constant
$$\sup_{x\in D} \|f(x) - f^\varepsilon(x)\| \leq C_1 \varepsilon \sup_{x\in D} \|f'(x)\|.$$
3. f of class $\mathcal{C}^2$, f^ε piecewise linear interpolation, C_2 a real constant
$$\sup_{x\in D} \|f(x) - f^\varepsilon(x)\| \leq C_2 \varepsilon^2 \sup_{x\in D} \|f''(x)\|.$$

In all these cases, it is true that f^ε converges uniformly to f with respect to ε, therefore f^ε satisfies the assumptions of Proposition 2.1.

2.5.2 Analysis of numerical convergence

We now consider the Euler-Maruyama method applied to the perturbed equation (49). We would like to find a balance between the error due to the numerical integration of the SDE with step size h and the approximation of the transport field f with f^ε. In this way, one can choose wisely the two parameters ε, h in order to avoid extra computational time.
Let us consider $X(t), X^\varepsilon(t)$ the solution of (48) and (49) respectively, and let us denote with X_n, X_n^ε the numerical solution obtained with Euler-Maruyama method applied to the two equations at time $t_n = hn, t_N = T$. It is known that if f is Lipschitz continuous with constant K, and if σ is a constant, then the strong error for X_n approximating $X(t)$ is given by (*e.g.*, [7, Chapter 10])

$$\sup_{n=0,\dots,N} \mathbb{E}\|X(nh) - X_n\| \leq Ch, \tag{52}$$

for a constant C independent of h. It is possible to obtain a similar estimate for X_n^ε estimating $X(t)$.

Proposition 2.2. *Let us consider* (48), (49) *with* $W_1 = W_2 = W$ *almost everywhere. Given* $h > 0$ *such that* $hN = T$ *for* $N \in \mathbb{N}^*$, *let us consider* X_n^ε *the numerical solution given by the Euler-Maruyama method applied to* (49), *i.e.,*

$$\begin{cases} X_{n+1}^\varepsilon = X_n^\varepsilon + f^\varepsilon(X_n^\varepsilon)h + \sigma(W(t_{n+1}) - W(t_n)), \quad n = 0, \dots, N-1, \\ X_0^\varepsilon = X_0. \end{cases}$$

Then, if f, f^ε *satisfy the assumptions 1. and 2. of Lemma 2.1*

$$\sup_{n=0,\dots,N} \mathbb{E}\|X(nh) - X_n^\varepsilon\| \leq Ch + \|f^\varepsilon - f\|_\infty \frac{e^{KT} - 1}{K}, \tag{53}$$

with C *a real constant independent of* h *and depending only on the final time* T *and the Lipschitz constant* K *of* f.

Proof. We consider X_n the numerical approximation of $X(t)$ obtained using Euler-Maruyama with the same initial condition X_0. If we add and substract X_n and apply the triangular inequality we obtain

$$\mathbb{E}\|X_n^\varepsilon - X(nh)\| \leq \mathbb{E}\|X_n^\varepsilon - X_n\| + \mathbb{E}\|X_n - X(nh)\|.$$

Since f is regular enough and σ is a constant, for the second term it is known that

$$\sup_{n=0,\dots,N} \mathbb{E}\|X_n - X(nh)\| \leq Ch. \tag{54}$$

We can then make a recursive analysis of the first term. For almost all ω

$$\begin{aligned}
\|X_n^\varepsilon - X_n\| &\leq \|X_{n-1}^\varepsilon - X_{n-1}\| + h\|f^\varepsilon(X_{n-1}^\varepsilon) - f(X_{n-1})\| \\
&\leq \|X_{n-1}^\varepsilon - X_{n-1}\| + h\|f^\varepsilon(X_{n-1}^\varepsilon) - f(X_{n-1}^\varepsilon)\| + h\|f(X_{n-1}^\varepsilon) - f(X_{n-1})\| \\
&\leq h\|f^\varepsilon - f\|_\infty + (1+hK)\|X_{n-1}^\varepsilon - X_{n-1}\| \\
&\leq h\|f^\varepsilon - f\|_\infty + (1+hK)(h\|f^\varepsilon - f\|_\infty + (1+hK)\|X_{n-2}^\varepsilon - X_{n-2}\|) \\
&\overset{(\cdots)}{\leq} h\|f^\varepsilon - f\|_\infty \sum_{i=0}^{n-1}(1+hK)^i + (1+hK)^n\|X_0^\varepsilon - X_0\|
\end{aligned}$$

Since $X_0^\varepsilon = X_0$ and using the geometric sum

$$\begin{aligned}
\|X_n^\varepsilon - X_n\| &\leq h\|f^\varepsilon - f\|_\infty \frac{(1+hK)^n - 1}{hK} \\
&\leq \|f^\varepsilon - f\|_\infty \frac{(1+hK)^N - 1}{K} \\
&\leq \|f^\varepsilon - f\|_\infty \frac{e^{KT} - 1}{K},
\end{aligned}$$

where the last inequality is valid since $N = T/h$ and K, T, h are all positive real numbers. Since the bound we found is independent of ω and n, we can take the expectation and the supremum, obtaining

$$\sup_{n=0,\dots,N} \mathbb{E}\|X_n^\varepsilon - X_n\| \leq \|f^\varepsilon - f\|_\infty \frac{e^{KT} - 1}{K}. \tag{55}$$

This result combined with (54) concludes the proof. □

As far as the weak convergence is concerned, it is known that the Euler-Maruyama method is of weak order one [7, Chapter 14]. The term due to the perturbation of the transport field can be treated as for the strong error, therefore we get without any further assumption for a constant C independent of h

$$\sup_{n=0,\dots,N} \|\mathbb{E}(X_n^\varepsilon - X(nh))\| \leq Ch + \|f^\varepsilon - f\|_\infty \frac{e^{KT} - 1}{K}.$$

Remark 2.3. If f^ε is the interpolation of f on a regular grid of size ε, the result of Proposition 2.2 allows to balance the interpolation error and the error due to numerical integration. In fact, we reported above some results on interpolation of f with piecewise polynomials f^ε, which we can plug in (53) as follows

1. if f is Lipschitz continuous of constant K or of class $\mathcal{C}^1$ and f^ε is piecewise constant, then

$$\sup_{n=0,\dots,N} \mathbb{E}\|X_n^\varepsilon - X(nh)\| = O(h) + O(\varepsilon).$$

2. if f is of class $\mathcal{C}^2$, and f^ε is piecewise linear, then

$$\sup_{n=0,\dots,N} \mathbb{E}\|X_n^\varepsilon - X(nh)\| = O(h) + O(\varepsilon^2).$$

Therefore, in the first case the step size h should be of the same order of magnitude as ε, while in the second case it should scale as ε^2.

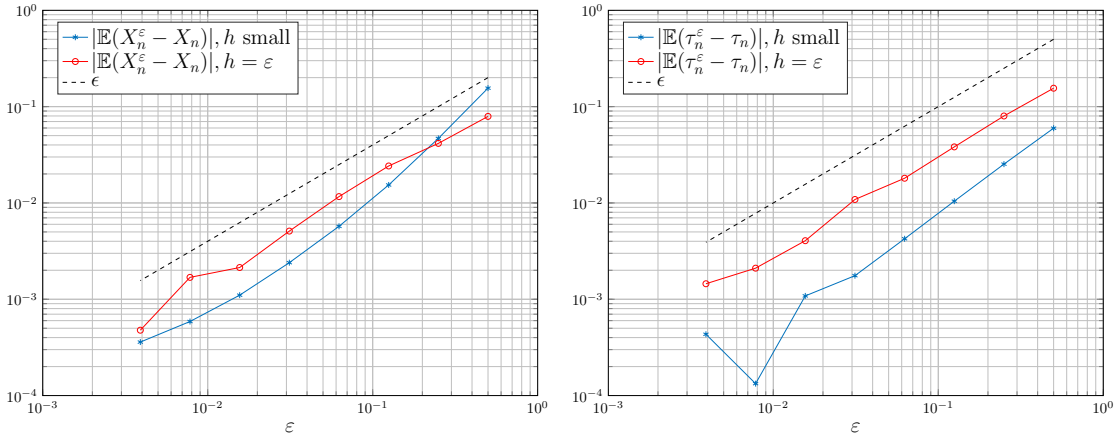

(a) Error on the solution.

(b) Error on the exit time.

Figure 13: Convergence of the numerical solution with respect to the interpolation characteristic size ε.

2.5.3 Numerical confirmation of the theory

We perform a numerical experiment in order to verify the theoretical bounds presented above. Let us consider the domain $D = [-1, 1]^2$ and the deterministic transport field given by

$$f(x, y) = \frac{1}{2}\left(x^2 + y^2, \quad |x - y|\right)^T.$$

In the domain, the transport field is Lipschitz continuous. Our aim is verifying whether the numerical solution computed using a piecewise constant interpolation of f leads to convergence with respect to the characteristic size of the grid used for interpolation. In the following, f^ε denotes the piecewise constant interpolation over D of f on a structured grid of equal size ε in both directions. Since the theoretical results interest the value of the solution itself and not the mean exit time from a domain, we start by considering the value itself. Then, we verify if the results are valid for the exit time as well.

Numerical solution. We consider the boundary conditions to be reflecting on all the boundary of D. We fix the parameters to be $T = 1, \sigma = 1$ and perform a Montecarlo simulation over $M = 10000$ simulations of Euler-Maruyama. Let us remark that since the boundary is completely reflecting, there is no distinction between CEM and DEM. Mantaining the notation of Proposition 2.2, we compute the weak error of X_n^ε with respect to X_n, which should be of order $O(\varepsilon)$. The reference solution X_n is computed over $N = 2^{10}$ timesteps over the time span. Then, we vary ε in the range $\varepsilon_i = 2^{-i}, i = 1, \dots, 8$ and compute the numerical solution X_n^ε either fixing the number of timesteps $N = 2^9$ or varying it so that $h_i = \varepsilon_i$, *i.e.*, the time and space discretizations have the same order of magnitude. In the first case, we wish to overkill the error due to numerical integration, while in the second case we wish to mantain an acceptable computational cost. Moreover, the bound presented in Remark 2.3 implies that theoretically the error should be independent of h, so we would expect similar results for both the approaches. Results (Figure 13a) confirm the theoretical results, with a clear rate of convergence equal to one, and the errors which are similar for the two approaches.

Mean exit time. We perform an experiment with the same values for all parameters as above, but we consider mixed killing and reflecting boundary conditions and we estimate the exit time τ. We wish that the theoretical results obtained for the solution apply practically to the exit time itself. We use the same strategies as above, either fixing a small step size h for any value of ε, or mantaining h equal to ε. Results (Figure 13b) show that the error is $O(\varepsilon)$ in both cases, with a smaller constant in case a small value of h is chosen. On the other side, we notice that fixing, *e.g.*, the error to 0.01, the computational time is in this case approximately sixteen times smaller in case h and ε are balanced.

Algorithm 2: Estimation of the exit time

Data: number of realizations M_r, number of trajectories M_t
Result: Estimate of the exit time $\bar{\tau}$
for $i = 1, \dots, M_r$ **do**
    Generate the random field A ;
    Find the solution of the Darcy problem ;
    Interpolate the velocity field on a structured grid of size Δ_u ;
    Estimate τ_i using CEM with step size Δ_u over M_t trajectories ;
end
$\tau = 1/M_r \sum_{i=1}^{M_r} \tau_i$;

2.6 Estimation of the exit time

The numerical and theoretical path we followed in the previous paragraphs enables us to build a Montecarlo simulation using which we estimate the mean exit time from a domain with the solution of the uncertain Darcy problem as a transport field. All consideration above allow us performing efficiently and accurately the estimation of the exit time *for each realization* of the Darcy problem. Therefore, it is sufficient to average over different realizations of the Darcy problem in order to obtain an estimation of the exit time, as in Algorithm 2. We consider the square domain $D = [-1, 1]^2$ and the following values for the parameters

- Random field: $\nu = 0.5, L_C = 0.05, \sigma_A = 1, \Delta_A = 0.0039$,
- Darcy problem: $p_0 = 1$,
- Finite Elements solution: $\Delta_p = 5 \cdot 10^{-3}$,
- Interpolation: $\Delta_u = 0.0625$,
- Trajectories: $X_0 = \begin{pmatrix} -0.8, & 0 \end{pmatrix}^T, T = 20$,

We vary the value of σ and generate 100 solutions of the Darcy problem for each value of σ, estimating the exit time with 10000 trajectories for each realization. The results we obtain are the following

σ	τ
$1 \cdot 10^{0}$	0.4718
$1 \cdot 10^{-1}$	3.9437
$1 \cdot 10^{-2}$	4.2634
$1 \cdot 10^{-3}$	3.9767
$1 \cdot 10^{-4}$	3.9906

We remark that in the transport-dominated case the exit time stabilizes on a value of approximately four seconds.

References

[1] M. Giles and K. Ramanan, *MLMC for Multi-Dimensional Reflected Diffusions*, in SIAM Conference on Uncertainty Quantification, 2016.

[2] E. Gobet, *Weak approximation of killed di usion using Euler schemes*, Stochastic Processes and their Applications, 87 (2000), pp. 167–197.

[3] E. Gobet, *Euler schemes and half-space approximation for the simulation of diffusion in a domain*, ESAIM: Probability and Statistics, 5 (2001), pp. 261–297.

[4] E. Gobet and S. Menozzi, *Stopped diffusion processes: boundary correction and overshoot*, Stochastic Processes and their Applications, 120 (2010), pp. 130–162.

[5] D. S. Grebenkov and R. Voituriez, *Exit time distribution in spherically symmetric two-dimensional domains*, (2014), pp. 1–34.

[6] D. J. Higham, X. Mao, M. Roj, Q. Song, and G. Yin, *Mean Exit Times and the Multilevel Monte Carlo Method*, SIAM/ASA Journal on Uncertainty Quantification, 1 (2013), pp. 2–18.

[7] P. E. Kloeden and E. Platen, *Numerical Solution of Stochastic Differential Equations*, Springer, 1992.

[8] S. Krumscheid, M. Pradas, G. A. Pavliotis, and S. Kalliadasis, *Data-driven coarse graining in action: Modeling and prediction of complex systems*, Physical Review E, 92 (2015), p. 042139.

[9] F. Nobile and F. Tesei, *A Multi Level Monte Carlo method with control variate for elliptic PDEs with log-normal coefficients*, Stochastic Partial Differential Equations: Analysis and Computations, (2015), pp. 1–47.

[10] G. A. Pavliotis, *Stochastic Processes and Applications*, Springer, 2014.

[11] P. E. Protter, *Stochastic Integration and Differential Equations*, Springer, second ed., 2004.

[12] A. Quarteroni, R. Sacco, and F. Saleri, *Numerical Mathematics*, Springer, 2007.

[13] L. Sirovich, J. E. Marsden, and S. S. Antman, *Theory and Applications of Stochastic Processes: An Analytical Approach*, vol. 170, Springer, 2010.